Engineering Innovations
ISSN: 2813-1002, Vol. 10, pp 3-14
doi:10.4028/p-7BWK6f

Submitted: 2023-10-24
Revised: 2023-11-03
Accepted: 2023-11-03
Online: 2024-04-03

Fracture Toughness Investigation of AL6082-T651 Alloy under Corrosive Environmental Conditions

Ibrahim Alqahtani[1,a*], Andrew Starr[1,b] and Muhammad Khan[1,c]

[1]School of Aerospace, Transport and Manufacturing, Cranfield University, Bedford MK43 0AL, UK

[a]I.Alqahtani@cranfield.ac.uk, [b]a.starr@cranfield.ac.uk, [c]muhammad.a.khan@cranfield.ac.uk

Keywords: Fracture toughness, Al6082 alloy, Corrosion, Temperature, Humidity

Abstract. The crack initiation and propagation in an aluminium alloy in a corrosive environment are complex because of the loading parameters and material properties, which may result in a sudden failure in real-time applications. This paper investigates the fracture toughness of aluminium alloy under varying environmental and corrosion conditions. The main objective of the work is to link the interdependencies of humidity and temperature for an AL6082-T651 alloy in a corrosive environment. This study investigates AL6082-T651alloy's fracture behaviour and mechanism through microstructure and fractographic studies. The results show that a non-corroded sample, at room conditions, provided more load-carrying capacity than a corroded sample. Additionally, an increase in temperature improves fracture toughness, while an increase in humidity results in a decrease in fracture toughness.

Introduction

Fracture toughness is a vital parameter that characterizes a material's ability to resist crack propagation. It can be quantified and standardized through experimental fracture mechanics techniques like structural integrity assessment, residual strength analysis, life service evaluation, and damage tolerance design for diverse engineering components and structures. Consequently, evaluating and testing fracture toughness has emerged as a crucial aspect in advancing the fracture mechanics approach and its engineering implementations. Standard terminology for fracture toughness testing and evaluation is specified by the American Society for Testing and Materials (ASTM) in E1823 and E399 [1–3]. A material's fracture toughness can also be affected by environmental factors such as humidity, temperature, and corrosion [4]. An environmental stress fracture is the general term in materials science used to refer to the premature failure of materials like metals, alloys [5], and composites due to tensile loads and environmental conditions. These fractures are induced by factors such as humid air, saltwater, and corrosive chemicals [6,7]. Many of these processes are also capable of affecting aluminium alloy and its composites [9, 8].

Al6082-T651 alloy is frequently employed as a structural material in numerous applications [7,10] due to its high specific strength among the 6xxx aluminium alloys [11]. Fracture toughness values can be used as a basis for material characterization, performance assessment, and quality assurance in common engineering structures like cars, ships, and aircraft. To store hydrogen in automobiles, high-pressure tanks made of an aluminium alloy and a layer wrapped in carbon fibre are now the most common option [12, 13]. However, high-pressure hydrogen can quickly impact the aluminium alloy, which causes its embrittlement to develop. When Aluminium alloys were subjected to a corrosive environment, 3.5% NaCl solution for 24 hours [14,15] and more, aluminium reacted with the water, causing hydrogen embrittlement (HE) [16]. In these samples, HE increases if subjected to high temperature, and when subjected to high humidity conditions causes its severity [18, 17]. High temperature, humidity, and applied load on the samples lead the hydrogen embrittlement and contribute to stress corrosion cracking (SCC). However, forming secondary phase particles in Al-Mg-Si alloys at high temperatures reduces the risk of hydrogen embrittlement and SCC in the 6xxx series compared with 7xxx aluminium alloys [19]. Hydrogen induced cracks will form in a material at critical temperatures and humidities because of the enriched hydrogen atoms near the crack tip [20].

Saudi Arabia is characterized by a desert climate with an extensive coastal area. The central region experiences sweltering and dry summers [21]. The humidity in the coastal area is high and oppressive. Its average monthly relative humidity in the Jeddah location, Riyadh, and Dhahran varies from 37% to 100. [21,22]. The surroundings in the coastal areas, such as temperature, humidity, and corrosive environment, affect aircraft components' conditions. Al-Mg-Si alloys were used in a helicopter rotor blade application [23–25]. The operation conditions of the rotor blade were affected by the surrounding environment, which encouraged corrosion. According to the failure analysis, corrosion of the threaded portion caused the failure to occur around the bolt hole [26–28].

There is still a need for a comprehensive approach to relate the interdependencies between couple loads, such as humidity and temperature of Al6082-T651 alloys in corrosive environments, which affect their properties[4]. Most investigations focused on studying aluminium alloys and their composites to determine their fracture toughness at room temperature and in the absence of humidity and corrosive environments. Additionally, it has been very uncommon to compare the effects of fracture toughness at various temperatures and humidity levels and their combined impact on the performance of AL6082-T651alloy. The temperature values are 20 oC, 40 oC, 60 oC, and 120oC, and the humidity levels are 40% to 90%, considered for experimentation.

In this paper, we investigated the effects of temperature and humidity on the fracture toughness of Al6082-T651 alloys. Using scanning electron microscopy (SEM), the fractographic characteristics of the Al6082-T651 alloy were studied to find the failure mechanism. Material selection and its properties, experimental procedures followed to pre-crack the specimen, immersion in a corrosive environment and thermal chamber, fracture toughness testing, and results and discussions are explained in subsequent sections.

Experimental Methods

Material

The AL6082-T651 alloy (also known as Al-Mg-Si-Mn) is a popular choice for structural applications due to its physical properties resembling Al6061 alloy [29]. Manganese is incorporated into the extruded medium to high-strength Al6082 alloy in T6 condition to enhance strain hardening, toughness, and strength through solution strengthening, while preserving ductility and corrosion resistance [30, 31]. The T651 state is achieved through solution treatment, stress relief by stretching, and artificial aging at approximately 180°, which prevents elastic recovery after processing. Tables 1 and 2 show, respectively, the chemical compositions and properties of AL6082-T651 alloy in the T651 condition. [29 - 32].

Table 1. Chemical composition of AL6082-T651 alloy (wt. %)

Element	Copper	Chromium	Manganese	Magnesium	Zinc	Titanium	Silicon	Iron	Aluminum
Wt.%	0.1	0.08	1.0	1.2	0.2	0.2	1.3	0.5	Balance

Table 2. Properties of AL6082-T651 alloy (wt. %)

Density (g/cc)	Tensile Strength (MPa)	Yield Strength (MPa)	Elastic Modulus (GPa)	Rigidity Modulus (GPa)	Hardness, Vickers	Elongation (%)
2.71	348	320	70	26.4	92	17.5

The AL6082-T651 alloy is designed to improve strength, toughness, elastic modulus, damage tolerance, and fatigue crack growth resistance. AL6082-T651 alloy is recommended for parts that need high strength and high toughness levels.

Specimen Preparation

The specimen utilized in this experiment to determine fracture toughness (KIc) is the compact tension (CT) specimen. Each AL6082-T651 alloy sample is machined as per the dimensions mentioned in the geometry given in Fig. 1. The notch in the centre of the specimen has been cut using the Wire cut EDM. The introduction of a fatigue crack was done using the INSTRON servo-hydraulic fracture toughness testing apparatus Moreover, in all CT specimens, a fatigue crack is introduced at

the notch's end while ensuring that the crack length to width (a/W) ratio remains at 0.54. Fracture toughness experimentation is carried out with a constant frequency of 3 Hz and by applying a cyclic load equivalent to 0.1 times the material's yield load. Fig. 2 shows the prepared sample, and Fig. 3 shows the experimental setup.

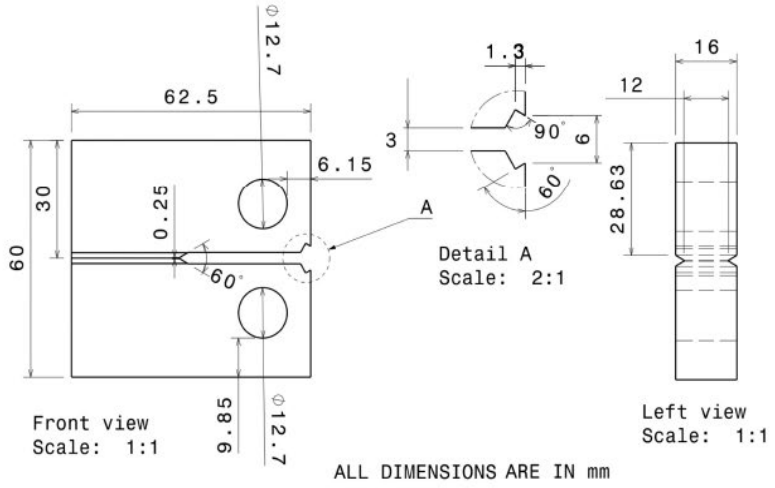

Fig. 1. The geometry of the CT specimen.

Fig. 2. Prepared CT specimens for fracture toughness test

Localized Corrosion

The AL6082-T651 alloy samples were suspended in a still solution of 3.5 wt.% NaCl aqueous solution for the localised corrosion tests. By taking into account the literature [33] and the ASTM G31 standard, the test duration—which is roughly 168 hours—has been calculated. Testing for static immersion corrosion was done in a room setting. Each of the pre-craked CT specimens shown in Fig. 3(b) was submerged in a 3.5 wt.% NaCl solution for 168 hours before being removed and allowed to dry in the air.

Fracture Toughness Test

The fracture toughness test was carried out for four different cases by considering the different testing environments as mentioned below:

Case i: Non-corroded and corroded specimens at temperature 20oC and humidity 40%.

Case ii: Corroded specimens at temperatures 40oC and 60oC, and humidity 40%.

Case iii: Corroded specimens at temperature and humidity (60oC & 80% and 120oC & 40%).

Case iv: Corroded specimens at temperature 20oC and humidity 70% and 90%.

In order to test the fracture toughness, a 0.1 mm/min displacement rate was maintained. The CT specimen's relative displacement of two knife edges was monitored during the fracture toughness test using a crack opening displacement (COD) gauge. To determine the fracture toughness of the AL6082-T651alloy, the load and displacement data are collected and subsequently analysed in accordance with standards [34]. Three specimens were tested for each condition, and the average fracture toughness value was taken into account.

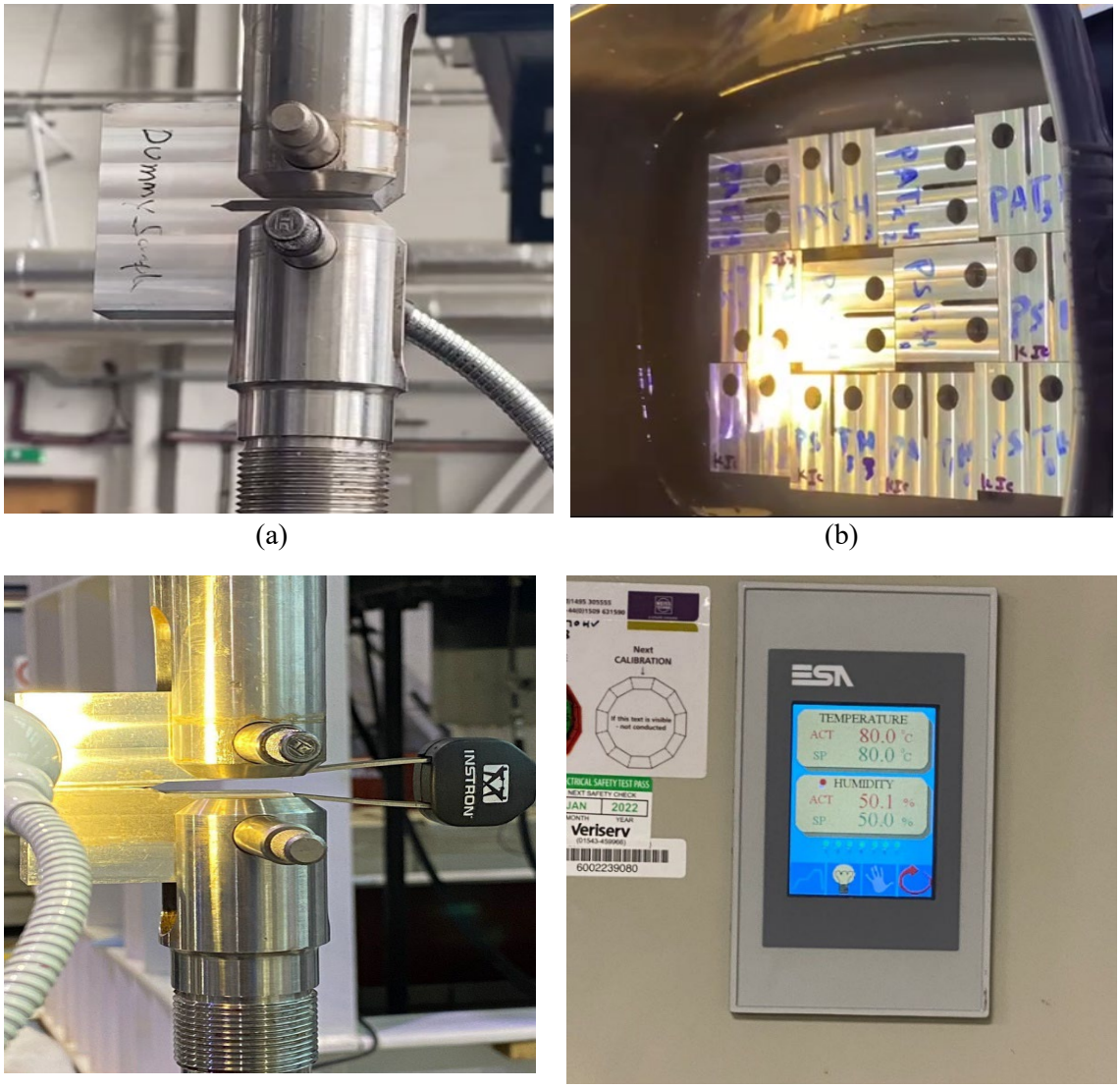

(a) (b)

(c) (d)

Fig. 3. Experimental setup: (a) Fatigue crack introduction to the CT specimen; (b) Immersion in 3.5% NaCl Solution; (c) Fracture toughness testing of the fatigue pre-cracked specimen with clip strain gauge; (d) Thermal Chamber used to maintain the required temperature and humidity

Results and Discussion

Microstructures and compositions

The microstructures of the SEM images of the AL6082-T651 alloy under various temperature and humidity conditions are shown in Fig. 4. The major influencing elements like Mg, Mn, and Si during exposure to different temperature and humidity conditions are shown in Fig. 4 (a-f). However, once the AL6082-T651 alloy is subjected to various temperature and humidity levels, oxide surfaces [35] start forming on their fractured surfaces, as seen in Fig. 4 (c-f). The presence of contents Mn and Mg show the alloying elements in the AL6082-T651alloy. In the compositions of the AL6082-T651 alloy at temperature 20oC, there is no oxide content in both uncorroded and corroded situations. However, the oxygen (O) content has been attained at higher temperatures and humidity levels. The content of O is due to the formation of oxides on the top surface of the fractured alloy.

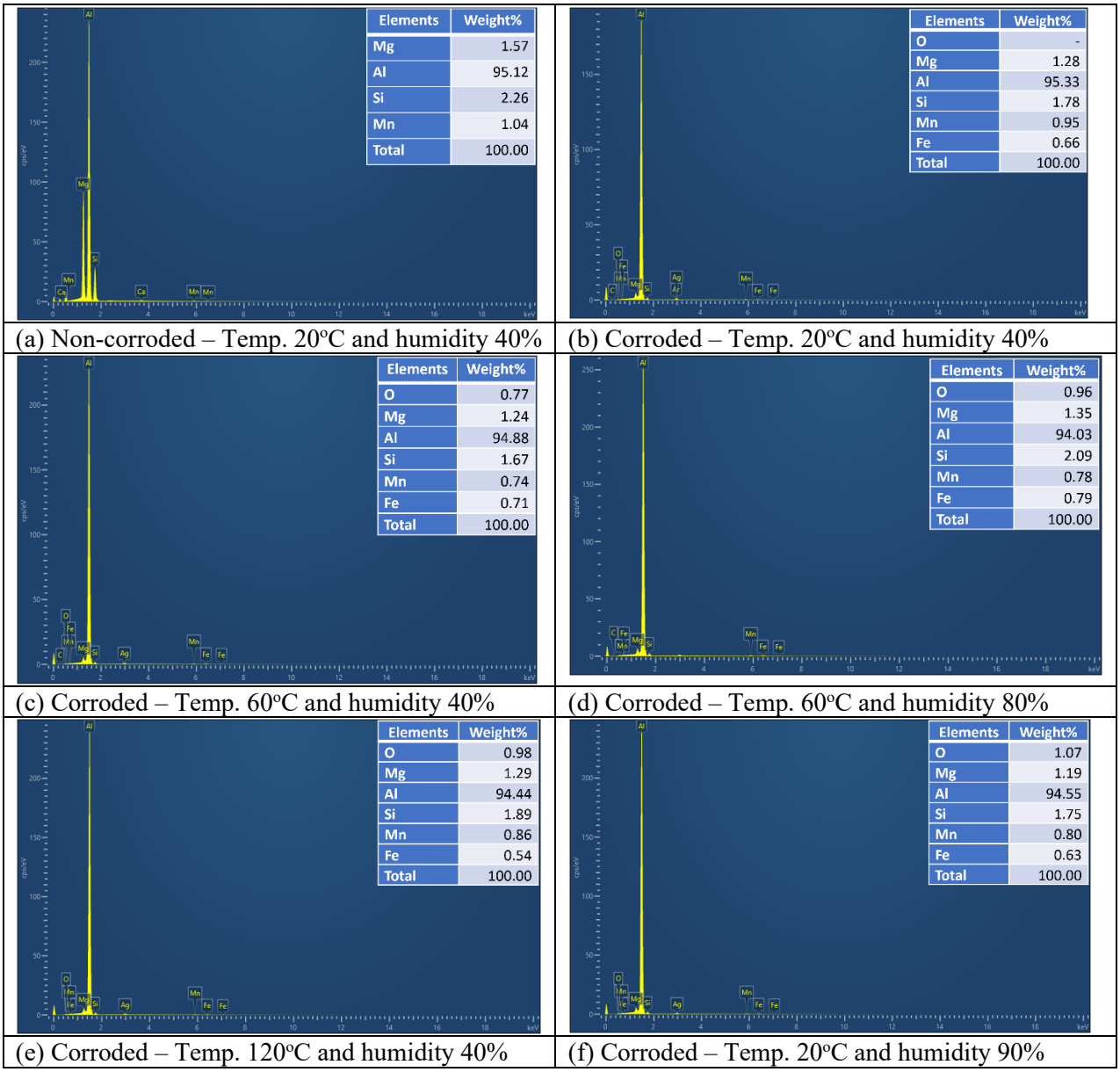

Fig. 4. EDS composition of specimen at different temperature and humidity levels

Fig. 5 from Energy Dispersive Spectroscopy (EDS) micrographs illustrates the mapping of Mg, Si, Mn, and other elements found in aluminium alloys. The EDS micrograph shows the mapping distribution of the elements of AL6082-T651 alloy for different temperature and humidity conditions. Along with Mg, Si and Mn, the presence of small O has also been identified for corroded samples. Exposure to a corrosive environment (168 hrs), different temperatures and humidity levels (72 hrs) form the oxide layer on the fractured surface of the AL6082-T651alloy. Since the exposure time is much less, the oxide layer formed is very thin, nearly 1%.

Load vs. COD

Fig. 6 displays the load variation versus crack opening displacement (COD) of the AL6082-T651 alloy under various temperature and humidity conditions. The alloy mentioned has a load-carrying capacity that decreases with rising humidity levels and rises with rising temperatures. The critical load (PQ) value can be calculated by drawing the 5% secant line to the maximum load (Pmax) on experimental data using the curve fitting phenomenon, as shown in Fig. 6. The plot shows that all cases' load vs COD curves follow the type III curve [34,36].

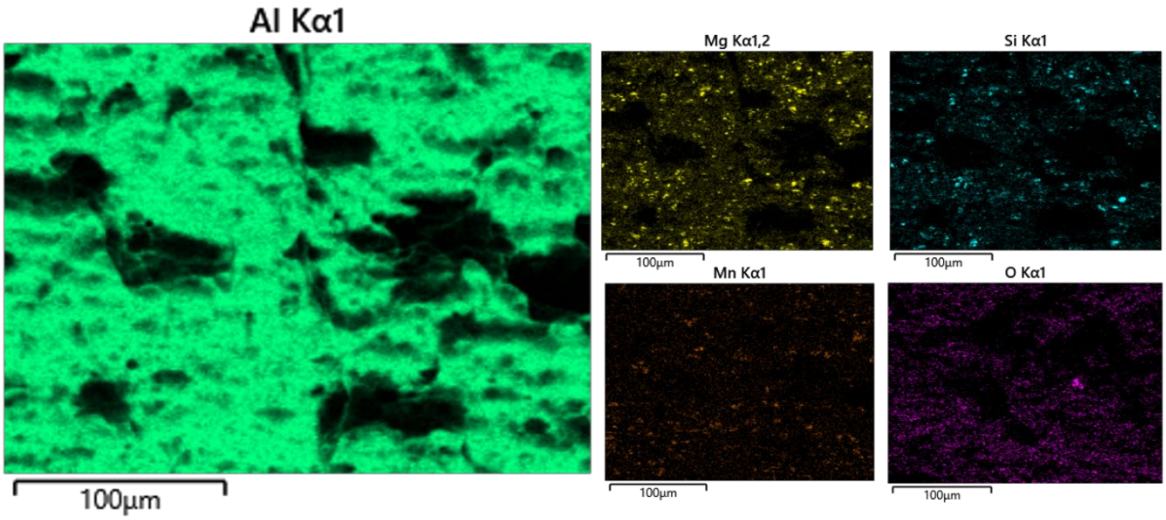

Fig. 5. EDS element mapping of AL6082-T651alloy: corroded samples at 120°C temperature and humidity 40%;

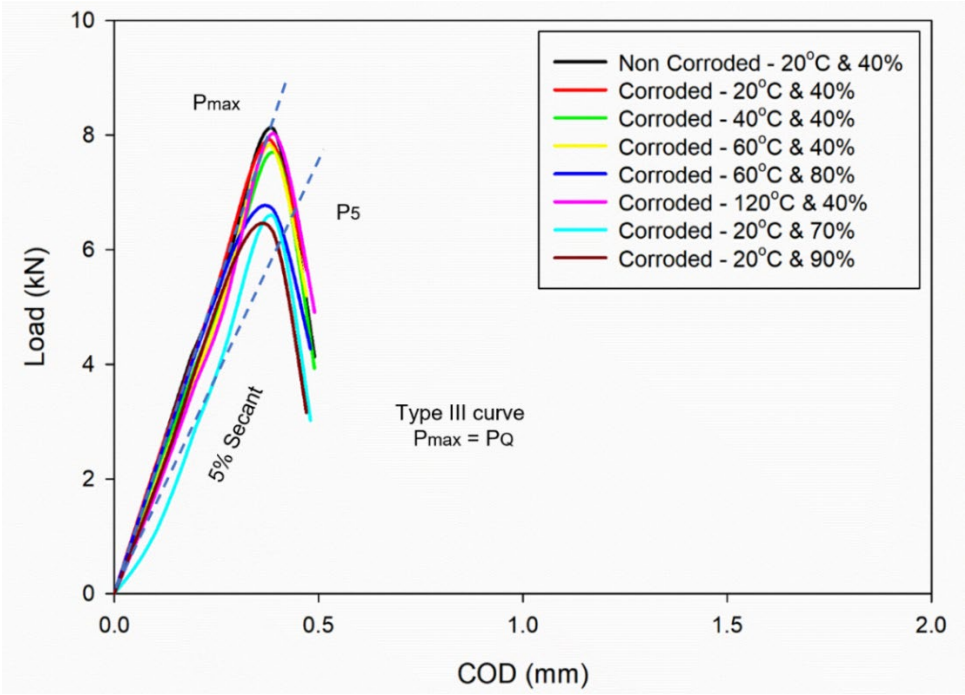

Fig. 6. Load vs COD graph of AL6082-T651alloy; (a-h) for various temperature and humidity conditions; (i) All conditions in one graph.

In the Type III condition, $P_Q = P_{max}$ applies where a specimen fails before exceeding 5% non-linearity. Conditional fracture toughness K_Q is computed from the P_Q value and the measured crack length for each test using the equation (1 and 2) [37].

$$K_Q = \frac{P_Q}{\sqrt{BB_N}\sqrt{W}} f\left(\frac{a}{W}\right) \tag{1}$$

Where for CT Specimens,

$$f\left(\frac{a}{W}\right) = \frac{\left(2+\frac{a}{W}\right)}{\left(1-\frac{a}{W}\right)^{3/2}}\left[0.886 + 4.64\left(\frac{a}{W}\right) - 13.32\left(\frac{a}{W}\right)^2 + 14.72\left(\frac{a}{W}\right)^3 - 5.6\left(\frac{a}{W}\right)^4\right] \tag{2}$$

Fracture Toughness

The fracture toughness is significantly influenced by the specimen thickness (B). The fracture toughness decreases as the specimen thickness increases. When the specimen thickness gets close to the critical limit, the fracture toughness value seems stable. Plane-strain fracture toughness [38],

denoted by K_{Ic}, is the name given to the estimated fracture toughness at this point. Equations (3 and 4) provide the conditions for the plane-strain fracture toughness [37]:

$$a, B \geq 2.5\left(\frac{K_Q}{\sigma_y}\right)^2 \tag{3}$$

$$W \geq 5.0\left(\frac{K_Q}{\sigma_y}\right)^2 \tag{4}$$

Plain strain fracture toughness requirements are met by the dimensions taken into consideration here [34]. Using Eq. (1), the fracture toughness of the AL6082-T651 alloy is calculated for a range of temperature and humidity conditions. Fig. 7 depicts how temperature and humidity affect the AL6082-T651alloy's fracture toughness. The graph demonstrates that while the material's fracture toughness decreases with an increase in humidity, it increases as the temperature rises.

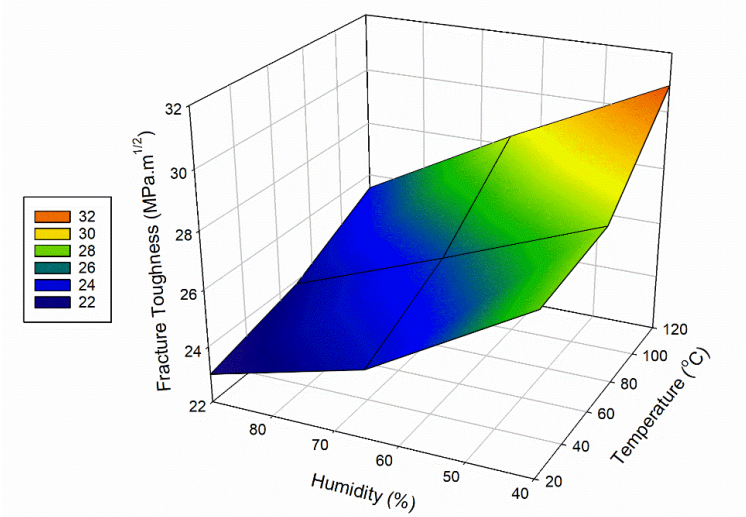

Fig. 7. Fracture toughness vs. temperature and humidity graph of AL6082-T651 alloy for various conditions

Fracture Surface Morphology

Fracture micrographs of the various CT specimens are obtained and are shown in Figs. 8 (a-f). Fig. 8 compares SEM micrographs of the fracture surfaces of smooth and notched specimens subjected to quasi-static strain rates. It was discovered that the core zone of the fracture surface featured dimples of varying heights and diameters. The high stress applied causes voids to form quickly during the nucleation stage. Large dimples are most likely produced by high uniaxial stress, which could accelerate the dimple fracture. The fracture surface's center zone exhibits ductile fracture filled with lumps and hollows. A typical nucleation-growth-coalescence phase of ductile fracture is depicted in Fig. 8 (a-f), where several voids and dimples may be seen. When a ductile material is subjected to uniaxial stress, micro-voids are formed in the core zone, prioritizing impurities like Mg, Si. As deformation progresses, the micro-voids continue to increase, eventually coalescing to produce numerous microcracks. The shear fracture occurs when the microcracks connect and grow to the vicinity of the specimen surface.

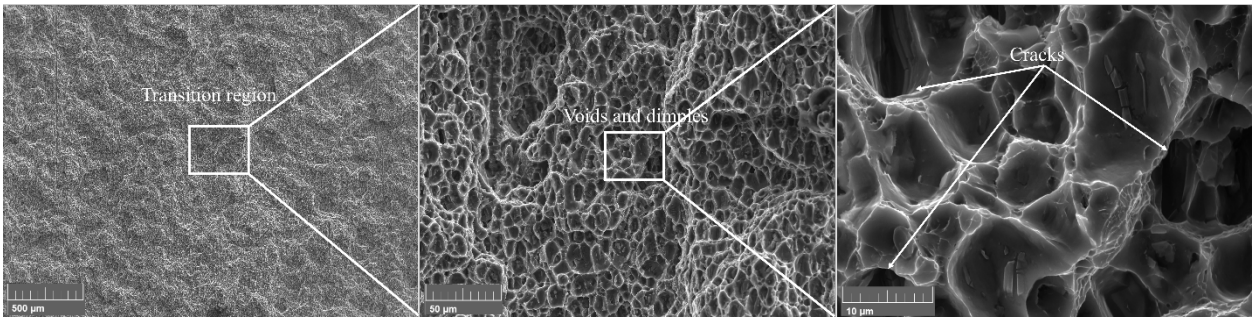

Fig. 8(a). SEM of fractured surface of non-corroded specimen at temperature 20ºC and humidity 40%.

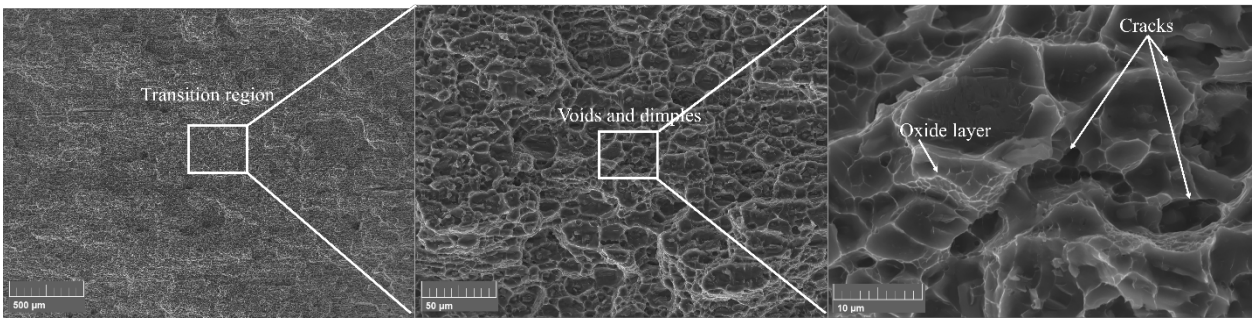

Fig. 8 (b). SEM analysis of a corroded specimen's fractured surface at 20°C and 40% humidity

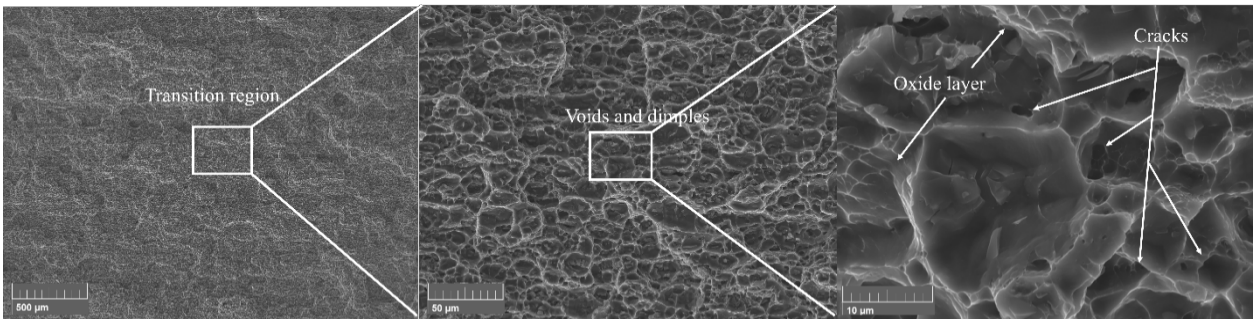

Fig. 8 (c). SEM analysis of a corroded specimen's fractured surface at 60°C and 40% humidity

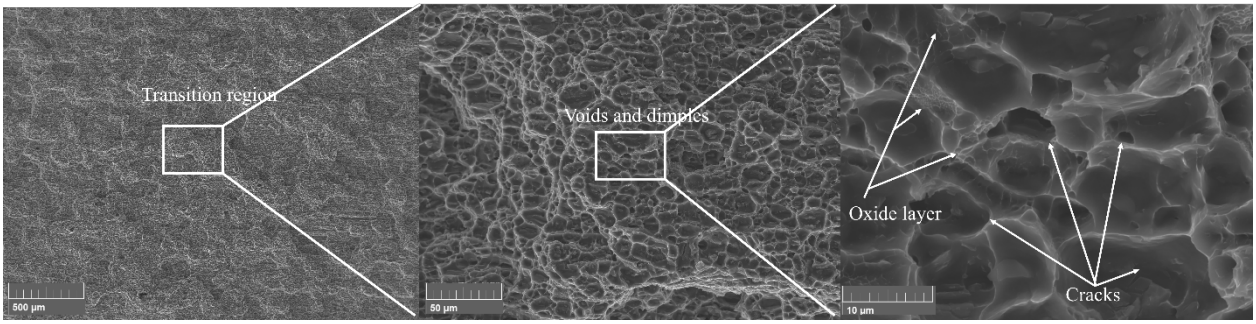

Fig. 8 (d). SEM analysis of a corroded specimen's fractured surface at 60°C and 80% humidity

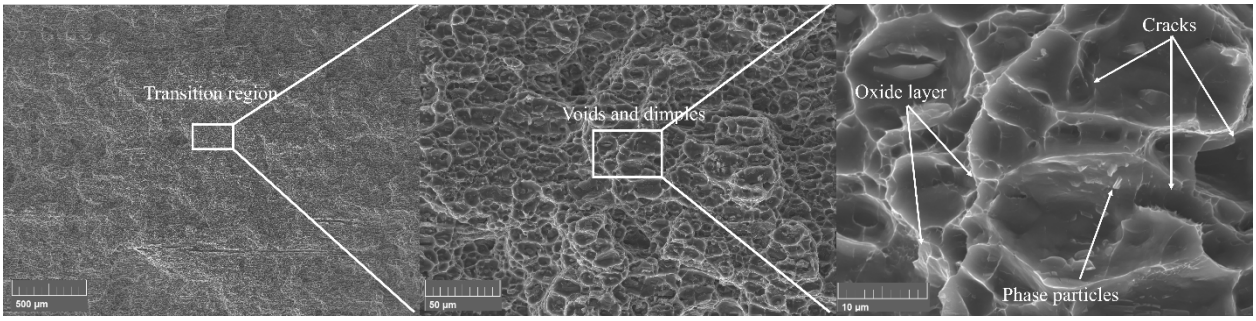

Fig. 8 (e). SEM analysis of a corroded specimen's fractured surface at 120°C and 40% humidity

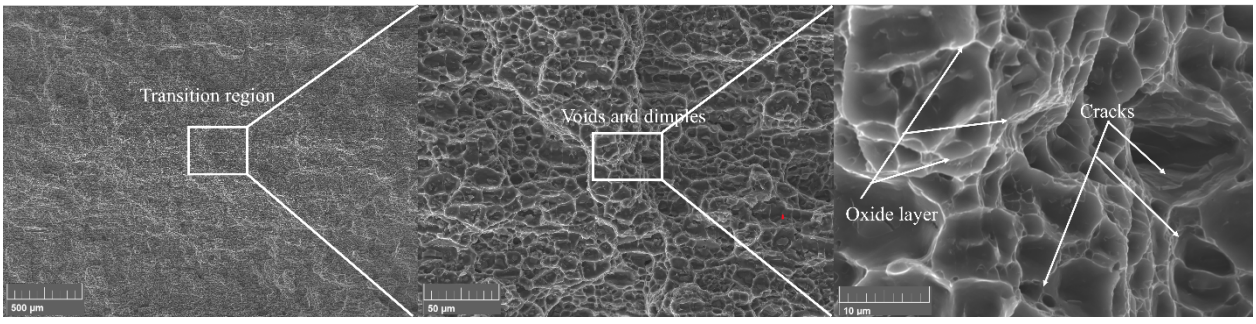

Fig. 8 (f). SEM analysis of a corroded specimen's fractured surface at 20°C and 90% humidity

Discussion

The experiments were conducted on four different cases, and the outcomes were presented in the following section.

Case i: Non-corroded and corroded specimens at temperature 20ºC and humidity 40%.

The load-carrying capacity for the non-corroded sample is higher than all other samples (Fig. 6. Since all other samples are tested under corroded conditions, the material's load-carrying capacity decreases. The peak load is about 8.12 kN for room conditions, which is 2.2% higher than the peak load of the corroded sample. The reduction in the 2.2% load-carrying capacity is small; however, it is obtained for the short period (168 hours) of sample immersion in the corrosive environment. This change in peak value is small due to the short-period corrosion effect on the sample. The corrosion environment has crucially affected the mechanical properties of the material. Due to corrosion, the material's surface reacts with the surrounding environment (oxygen and room humidity) and forms the oxide layers. The formation of oxide layers increases the crack nucleation and thus reduces the fracture toughness.

Large dimples on the rough fracture surfaces indicate a ductile fracture, which suggests the fracture process in each case was caused by void coalescence. Under various testing settings, void development and coalescences cause the dimples to form. In all the cases, the transition zone is evident as depicted. These locations correspond to the matrix's local embitterment or restricted plastic deformation in Figs. 8 (a) and 8 (b), there is no sign of quasi-cleavage fracture that may be observed [39]. The non-corroded specimen fails to be completely ductile in nature under room conditions and is characterized by voids and dimples shown in Fig. 8 (a). The fracture surface of the corroded sample, shown in Fig. 8 (b), shows the formation of single-mode fracture, i.e., voids and dimples, and there is no sign of brittle failure. However, the little oxide layer can be observed.

Case ii: Corroded specimens at temperatures 40oC and 60oC, and humidity 40%.

At 40°C and 60°C, the corroded sample has nearly the same load-carrying capacity. The percentage of the alloy's elongation increases as temperature rises from room temperature to 60oC [40]. As a result, as the temperature rises, the material becomes more ductile, which in turn makes it harder to fracture. The cracked surface of the AL6082-T651 alloy is subjected to plastic deformation at 60°C temperature during crack propagation, which causes a thin layer of the oxide layer to form [35]. The microstructure shown in Fig. 4 (c) and Fig. 8 (c) also displays the formation of the oxide layer.

Case iii: Corroded specimens at temperature and humidity (60oC & 80% and 120oC & 40%).

The load carrying capacity for the corroded sample at temperature 60ºC and humidity 80% is 6.69kN, shown in Fig. 6, whereas for temperature 120oC and humidity 40%, the load carrying capacity decreases by 16 %. The corroded sample at a temperature of 120oC and room humidity has a higher load carrying capacity than the combined temperature of 60oC and humidity condition of 80%.

At a temperature of 120oC, a thin oxide layer has been observed acting as crack closure [41]. The development of crack closure lessens the likelihood of crack propagation, increasing the material's ability to support more weight. At the high temperature depicted in Fig. 7, the crack toughness of the alloy increases because of the crack closure and increased ductility. The EDS analysis of the particles in Fig. 4 and 5 revealed that those phases typically contain a significant amount of Fe, as shown in Fig. 4 (b-f), in addition to Al, Si, Mg, and Mn. These particles might be therefore recognized as AlMg(Fe3Mn2)Si phase [42] (EDS plot in Fig. 4). The mapping of these phase particles is also shown in Fig 8(e). The amount of Mn and Mg elements present affects the morphology of the AlMg(Fe3Mn2)Si phase. Higher hardness and less ductility are the results of these phase particles. As a result, the material's ability to support more weight is reduced, which lowers fracture toughness.

Case iv: Corroded specimens at temperature 20oC and humidity 70% and 90%.

The load-carrying capacity for the corroded sample at room temperature and humidity at 70% is 6.09 kN, whereas it is reduced for 90% humidity. Fig. 6 (g) shows the load vs COD plot, which offers some non-linearity due to the higher humidity. Fig. 6 shows that the corroded samples' load-carrying

capacity and fracture toughness under high humidity conditions is 24.2% lower than that of the corroded samples at room conditions. The formation of oxide layers, loss of ductility due to corrosion, and increased crack initiation were the reasons for the decrement in fracture toughness. Fig. 8 (f) illustrates the creation of brittle features such as voids, deeper dimples, and oxide layers on the fracture surfaces at the notch area of the CT specimen in a high-humidity environment. Early crack propagation brought on by the crack nucleation lowers the material's threshold fracture toughness. As a result, as the corrosive environment, such as humidity, increases, the AL6082-T651 alloy's plain strain fracture toughness decreases.

Conclusions

The paper explores the impact of localized corrosion on the fracture toughness of AL6082-T651 alloy at various temperatures and humidity levels. The investigation involves experiments and fractographic studies. The following conclusions are made based on the examinations:

- The load-carrying capacity of the non-corroded sample, at room conditions, is 3% higher than the corroded sample. The fractured surfaces show no sign of brittleness and a little oxide layer formation.
- As the temperature increases, the percentage elongation of the aluminum alloy also increases, from 20°C to 120°C, enhancing the material's ability to withstand fracture. At high temperatures and humidity levels, the pre-cracked surface of AL6082-T651 alloy is subjected to forming a very thin oxidized layer.
- The increment in humidity, from 40% to 90% at temperature 20oC, forms an oxide layer, loss of ductility due to corrosion, formation of hard AlMg(Fe3Mn2)Si phases, and increased crack initiation and thus, reducing the fracture toughness by 12.5% than that of the corroded samples at room conditions.

Furthermore, from the conclusions, it is recommended to investigate the fracture toughness of AL6082-T651alloy, considering the implications in the coastal region.

References

[1] Anderson TL. Fracture mechanics – fundamentals and applications. 3rd edn. Boca Raton: CRC Press; 2005.

[2] Kamei K, KM. Investigating the Structural Dynamics and Crack Propagation Behaviour under Uniform and Non-Uniform Temperature Conditions. Materials (Basel). 2021; 14(22): 7071. Available at: DOI:doi: 10.3390/ma14227071.

[3] Raviraj MS, Sharanaprabhu CM, Mohankumar GC. Experimental investigation of effect of specimen thickness on fracture toughness of Al-TiC composites. Frattura ed Integrita Strutturale. 2016; 10(37): 360–368. Available at: DOI:10.3221/IGF-ESIS.37.47

[4] Ibrahim M Alqahtani, Andrew Starr, Mohammad Khan. Experimental and theoretical aspects of crack assisted failures of metallic alloys in corrosive environments – A review. Materials Today: Proceedings. 2022; 66: 2530–2535. DOI:https://doi.org/10.1016/j.matpr.2022.07.075

[5] Ibrahim M Alqahtani, Andrew Starr, Mohammad Khan. (2023) Coupled Effects of Temperature and Humidity on Fracture Toughness of Al–Mg–Si–Mn Alloy. Materials (Basel) 16:. Journal Pre-proof 20 https://doi.org/https://doi.org/10.3390/ma16114066.

[6] Cavalcante TRF, Pereira GS, Koga GY, Bolfarini C, Bose WW, Filho JAA. Fatigue crack propagation of aeronautic AA7050-T7451 and AA2050-T84 aluminum alloys in air and saline environments. International Journal of Fatigue. 2022; 154(106519). DOI:https://doi.org/10.1016/j.ijfatigue.2021.106519

[7] Muñoz AF, Buenhombre JLM, García-Diez AI, Fabal CC, Díaz JJG. Fatigue Study of the Pre-Corroded 6082-T6 Aluminum Alloy in Saline Atmosphere. Metals. 2020; 10: 1260. Available at: DOI:https://doi.org/10.3390/met10091260

[8] Ramakrishna Hegde, Sivaram NM, Ajaykumar BS, LJK. Evaluation of Heat Treatment Effect on Fracture Behavior of Aluminum Silicon Carbide Graphite Hybrid Composite. International Journal of Applied Engineering Research. 2017; 12(5): 605–610.

[9] Zhu X, Jones JW, JEA. Effect of Frequency, Environment, and Temperature on Fatigue Behavior of E319 Cast-Aluminum Alloy: Small-Crack Propagation. Metallurgical and Materials Transactions A. 2008; 39A: 2666–2680. Available at: DOI:10.1007/s11661-008-9630-2

[10] Correia JAFO, De Jesus AMP, Alves ASF, Lesiuk G, Tavares PJS, Moreira PMGP. Fatigue crack growth behaviour of the 6082-T6 aluminium using CT specimens with distinct notches. Procedia Structural Integrity. Elsevier B.V.; 2016; 2: 3272–3279. Available at: DOI:10.1016/j.prostr.2016.06.408

[11] Saleemsab Doddamani, Mohamed Kaleemulla. Fracture toughness investigations of Al6061-Graphite particulate composite using compact specimens. Frattura ed Integrità Strutturale. 2017; 41: 484–490. Available at: DOI:10.3221/IGF-ESIS.41.60

[12] Chen Yizhe, Shilong Zhao, Huijuan Ma, Hui Wang, Lin Hua SF. Analysis of Hydrogen Embrittlement on Aluminum Alloys for Vehicle-Mounted Hydrogen Storage Tanks: A Review. Metals. 2021; 11(8): 1303. Available at: DOI:https://doi.org/10.3390/met11081303

[13] Urbanczyk R, Peinecke K, Felderhoff M, Hauschild K, Kersten W, Peil DB. Aluminium alloy based hydrogen storage tank operated with sodium aluminium hexahydride Na3AlH6. International Journal of Hydrogen Energy. 2014; 39(30): 17118–17128. DOI: https://doi.org/10.1016/j.ijhydene. 2014.08.101

[14] Albrecht J, Bernstein IM, AWT. Evidence for dislocation transport of hydrogen in aluminum. Metall. Mater. Trans. A. 1982; 13: 811–820.

[15] Bochkaryova AV, Li YV, Barannikova SA, Zuev LB. The effect of hydrogen embrittlement on the mechanical properties of aluminum alloy. IOP Conference Series: Materials Science and Engineering. 2015; 71(1). DOI:10.1088/1757-899X/71/1/012057

[16] Dwarakadasa ES, RA. Effect of hydrogen in aluminium and aluminium alloys: A review. Bull. Mater. Scl. 1990; 19(1): 103–114.

[17] Safyari M, Hojo T, Moshtaghi M. Effect of environmental relative humidity on hydrogen-induced mechanical degradation in an Al–Zn–Mg–Cu alloy. Vacuum. Elsevier Ltd; 2021; 192(July): 110489. DOI:10.1016/j.vacuum.2021.110489

[18] Safyari M. Microstructure Effects on Hydrogen Trapping and Associated Mechanical Degradation in High Strength Aluminum Alloys. Tohoku University; 2022. DOI: http://hdl.handle.net/10097/00135880

[19] Takeshi Ogawa, Shota Hasunuma, Toshiki Shirawachi, NF. Effect of Chemical Composition and Relative Humidity on the Humid Gas Stress Corrosion Cracking of Aluminum Alloys. Journal of High Pressure Institute of Japan. 2019; 57(1): 24–33.

[20] Scully JR, Young GA, Smith SW. Hydrogen embrittlement of aluminum and aluminum-based alloys. Gaseous Hydrogen Embrittlement of Materials in Energy Technologies: The Problem, its Characterisation and Effects on Particular Alloy Classes. 2012; : 707–768. DOI:https://doi.org/10.1533/9780857093899.3.707.

[21] Alrashed F, Asif M. Climatic Classifications of Saudi Arabia for Building Energy Modelling. Energy Procedia. Elsevier B.V.; 2015; 75: 1425–1430. Available at: DOI:10.1016/j.egypro.2015.07.245

[22] Climatemp. Relative Humidity in Riyadh, Saudi Arabia. 2022. DOI: http://www.riyadh.climatemps.com/humidity.php

[23] Amura M, Aiello L, Colavita M, De Paolis F, Bernabei M. Failure of a Helicopter Main Rotor Blade. Procedia Materials Science. Elsevier B.V.; 2014; 3: 726–731. DOI:10.1016/j.mspro.2014.06.119

[24] Romeyn A. Main rotor blade failure analysis report. 2005.

[25] Inc. SH. In-Flight Separation of Main Rotor Blade and Collision with Terrain. 2011; (November).

[26] Kieselbach R, Soyka G. Failure of a helicopter rotor, Technology, Law and Insurance. T and F Online. 2000; 5(3–4): 141–146.

[27] Klysz S, Lisiecki J, Kurdelski M. Material testing of the helicopter main rotor blades. 37th Solid Mechanics Conference. 2010.

[28] Saleemsab Doddamani, Wang C, Mohamed MJ, Arefinkowser M. Fracture analysis of aa6061-graphite composite for the application of helicopter rotor blade. Frattura ed Integrita Strutturale. 2021; 15(58): 191–201. DOI:10.3221/IGF-ESIS.58.14

[29] Moreira PMGP, Jesus AMP, Ribeiro AS, Castro PMST. Fatigue crack growth in friction stir welds of 6082-T6 and 6061-T6 aluminium alloys: A comparison. Theoretical and Applied Fracture Mechanics. 2008; 50(2): 81–91.

[30] Lina M, Shehadeh ISJ. The Effect of Adding Different Percentages of Manganese (Mn) and Copper (Cu) on the Mechanical Behavior of Aluminum. Jordan Journal of Mechanical and Industrial Engineering. 2016; 10(1): 19–26.

[31] Davis JR. Aluminum and Aluminum Alloys. Metals Handbook Desk Edition. 2nd edn. ASM International; 1998. pp. 417–505.

[32] Moreira PMGP, Santos T, Tavares SMO, Richter-Trummer V, Vilaça P, Castro PMST. Mechanical and metallurgical characterization of friction stir welding joints of AA6061-T6 with AA6082-T6. Materials & Design. 2009; 30(1): 180–187.

[33] Zakaria HM. Microstructural and corrosion behavior of Al/SiC metal matrix composites. Ain Shams Engineering Journal. 2014; 5: 831–838.

[34] ASTME399-22. Standard test method for linear-elastic plane strain fracture toughness KIc of metallic materials. American Society for Testing and Materials. 2022.

[35] Jian Pu, Yali Zhang, Xiaogang Zhang, Xinlu Yuan, Pingdi Ren ZJ. Mapping the fretting corrosion behaviors of 6082 aluminum alloy in 3.5% NaCl solution. Wear. 2021; 482–483(203975): 1–11. DOI:https://doi.org/10.1016/j.wear.2021.203975

[36] Zhu XK, Joyce JA. Review of fracture toughness (G, K, J, CTOD, CTOA) testing and standardization. Engineering Fracture Mechanics. 2012; 85: 1–46. DOI:10.1016/j.engfracmech. 2012.02.001

[37] Zhu Xian-Kui, Joyce JA. Review of fracture toughness (G, K, J, CTOD, CTOA) testing and standardization. Engineering Fracture Mechanics. 2012; 85: 1–46. DOI:10.1016/j.engfracmech.2012.02.001

[38] Raviraj MS, Sharanaprabhu CM, GCM. Experimental investigation of effect of specimen thickness on fracture toughness of Al-TiC composites,. Frattura ed Integrità Strutturale. 2016; 37: 360–368. DOI:10.3221/IGF-ESIS.37.47

[39] Ibrahim M Alqahtani, Andrew Starr, Mohammad Khan. Investigation of the Combined Influence of Temperature and Humidity on Fatigue Crack Growth Rate in Al6082 Alloy in a Coastal Environment. Materials 2023, 16, 6833. https://doi.org/10.3390/ma16216833

[40] Delshad Gholami M, Hashemi R, MS. The effect of temperature on the mechanical properties and forming limit diagram of aluminum strips fabricated by accumulative roll bonding process. Journal of Materials Research and Technology. 2020; 9(2): 1831–1846. DOI:https://doi.org/10.1016/j.jmrt.2019.12.016.

[41] Suresh S; Zamiski GF, Ritchie DRO. Oxide-Induced Crack Closure: An Explanation for Near-Threshold Corrosion Fatigue Crack Growth Behavior. Metallurgical and Materials Transactions A. 1981; 12(8): 1435–1443. DOI:10.1007/bf02643688

[42] Mrówka-Nowotnik G, Sieniawski J, MW. Intermetallic phase particles in 6082 aluminium alloy. Archives of Materials Science and Engineering. 2017; 28(2): 69–76.